Compositional variability in lavas from the Ontong Java Plateau: results from basalt clasts within the volcaniclastic succession at Ocean Drilling Program Site 1184

JOHN T. SHAFER[1], CLIVE R. NEAL[1] & PATERNO R. CASTILLO[2]

[1]*Department of Civil Engineering and Geological Sciences, University of Notre Dame, 156 Fitzpatrick Hall, Notre Dame, IN 46556, USA (e-mail: jshafer@nd.edu)*

[2]*Geosciences Research Division, Scripps Institution of Oceanography, University of California, San Diego, La Jolla, CA 92093-0212, USA*

Abstract: Tholeiitic basalts have been recovered from drill sites in different locations on the Ontong Java Plateau (OJP) and are remarkably homogeneous across this large igneous province. The most abundant basalt type is represented by the Kwaimbaita Formation on Malaita in the Solomon Islands, where it is capped by the isotopically distinct and slightly more incompatible-element-enriched basalt of the Singgalo Formation. Ocean Drilling Program (ODP) Leg 192 drilled five sites on the OJP, four of which penetrated basement lava successions. All basalt recovered during Leg 192 is chemically and isotopically indistinguishable from Kwaimbaita-type lavas.

Site 1184 of ODP Leg 192 is situated on the eastern salient of the OJP, and is unique because the recovered volcaniclastic succession contains the first conclusive evidence for emergence of part of the OJP above sea level. Within this succession are clasts of basaltic material. We report the major element-, trace-element and isotopic compositions of 14 moderately to highly altered basalt clasts. On the basis of incompatible-element concentrations, specifically high field strength elements (HFSE) and rare earth elements (REE), four groups of clasts are defined. Group 1 clasts are similar to basalt from the Kwaimbaita Formation. Group 2 clasts show variable composition, but the heavy rare earth element (HREE) concentrations are similar to those of basalts from the Kwaimbaita Formation. Group 3 clasts have compositions similar to the high-MgO Kroenke-type basalt recovered during ODP Leg 192. Group 4 clasts are more evolved than the Kwaimbaita or Singgalo lavas, and contain deep negative Eu and Sr anomalies on primitive-mantle (PM)-normalized diagrams, as well as high concentrations of Nb, Ta and Th. Group 4 clasts also show a large fractionation of Nb from La and have $(Nb/La)_{PM}$ ratios of approximately 2. Sr-, Nd- and Pb-isotope ratios were measured on five clasts covering all four groups. Although the Sr- and Pb-isotope ratios exhibit some variability, which we attribute to alteration, the Nd-isotope ratios are within the field defined for Kwaimbaita-type lavas.

We conclude that most of the compositional variability displayed by these clasts is a result of alteration and that Ta appears to be the most immobile incompatible trace element. All of the clasts were derived from the mantle source that produced the Kwaimbaita-type and Kroenke-type basalts. Our data emphasize the widespread nature of Kwaimbaita-type basalt and show that the source region was active under both the eastern salient and the high plateau of the OJP.

The Ontong Java Plateau (OJP) is the largest of the Earth's large igneous provinces (LIPs) and covers an area of approximately 2.0×10^6 km^2. The OJP was emplaced rapidly, primarily around 122 Ma, with a possible second plateau-building event at about 90 Ma (e.g. Mahoney *et al.* 1993; Tejada *et al.* 1996, 2002). The *c.* 122 Ma event produced two geochemically similar, but isotopically distinct, lava types that were originally recognized in Unit A and Units C–G, respectively, from the Ocean Drilling Program (ODP) Leg 130 Site 807 (Mahoney *et al.* 1993). Thicker basalt sequences with similar compositions to the Unit A and Units C–G groups were described by Tejada *et al.* (2002) from subaerial outcrops on Malaita, Solomon Islands. These sequences were called the Singgalo Formation (compositionally equivalent to Unit A) and the Kwaimbaita Formation (compositionally equivalent to Units C–G). The presence of these two groups on both the northern and southern margins of the OJP, some 1200 km apart, is a testament to the size of the magmatic event(s) that produced the OJP. Singgalo-type basalt is slightly more enriched in incompatible elements than is Kwaimbaita-type basalt, and it is also

From: FITTON, J. G., MAHONEY, J. J., WALLACE, P. J. & SAUNDERS, A. D. (eds) 2004. *Origin and Evolution of the Ontong Java Plateau.* Geological Society, London, Special Publications, **229**, 333–351. 0305-8719/$15.00

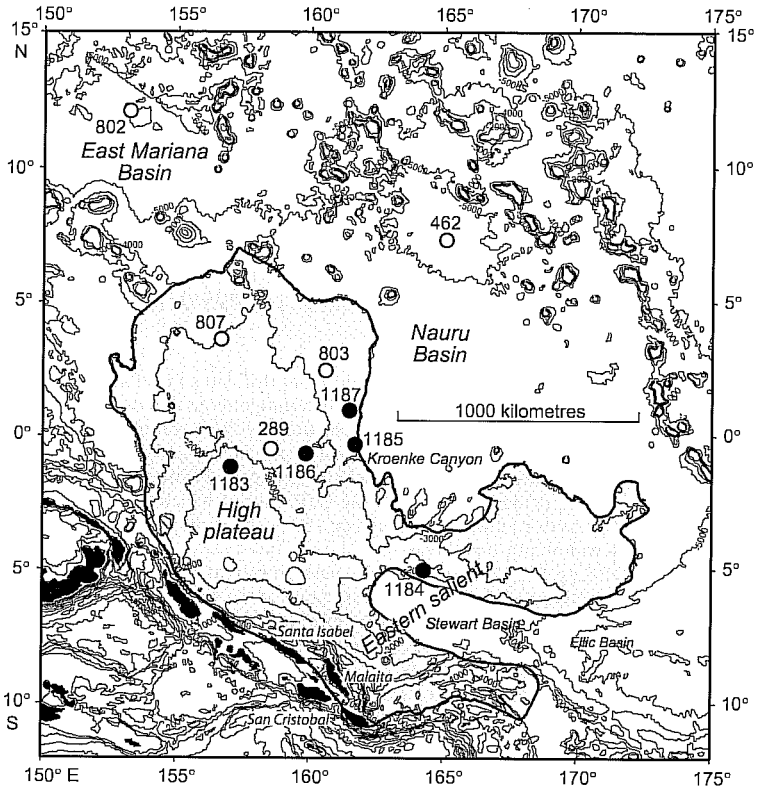

Fig. 1. Bathymetric map of the Ontong Java Plateau and surrounding area showing the locations of basement drill sites. Modified from Mahoney *et al.* (2001).

isotopically distinct. It has lower initial ε_{Nd} (relative to chondritic uniform reservoir, Chur) (+3.8–+5.4 v. +5.4–+6.5) and present-day $^{206}Pb/^{204}Pb$ (18.245–18.521 v. 18.626–18.708), and slightly higher initial $^{87}Sr/^{86}Sr$ (0.7040–0.7042 v. 0.7034–0.7039) than Kwaimbaita-type basalt (e.g. Mahoney 1987; Mahoney & Spencer 1991; Mahoney *et al.* 1993; Tejada *et al.* 1996, 2004).

Site 1184 of ODP Leg 192 is located on the unnamed northern ridge of the eastern salient of the OJP (Fig. 1). Until Leg 192, the relationship of the eastern salient to the main or high plateau was unknown (Mahoney 1987; Richards *et al.* 1989). Kroenke & Mahoney (1996) and Tejada *et al.* (1996) speculated that the eastern salient might specifically be the locus of the *c.* 90 Ma eruptions, whereas Mahoney *et al.* (2001) suggested that it could be either part of the main plateau or a product of the plume tail after main plateau emplacement. At about 90 Ma, the eastern salient may have been rifted into northern and southern lobes during more than 300 km of N–S extensional tectonism and rifting associated with the opening of the Ellice and Stewart basins (Fig. 1) (Neal *et al.* 1997). This poorly understood rifting event may also have contributed to the magmatic development of the volcaniclastic succession at Site 1184. Biostratigraphic information indicates a middle Eocene age (42–45 Ma) (Mahoney *et al.* 2001; Bergen 2004; Sikora & Bergen 2004); however, recent $^{40}Ar/^{39}Ar$ dating of Site 1184 plagioclase crystals has produced an estimated eruption age of 123.5 ± 1.8 Ma (Chambers *et al.* 2004).

One of the most significant results from ODP Leg 192 was that Site 1184 provides the first clear evidence of emergence of any part of the OJP above sea level (Mahoney *et al.* 2001; Thordarson 2004). Wood fragments were found at the boundaries between four of the six subunits within the volcaniclastic succession at Site 1184. The presence of oxidized horizons in subunit IIC probably indicates subaerial exposure (see Mahoney *et al.* 2001; Thordarson 2004).

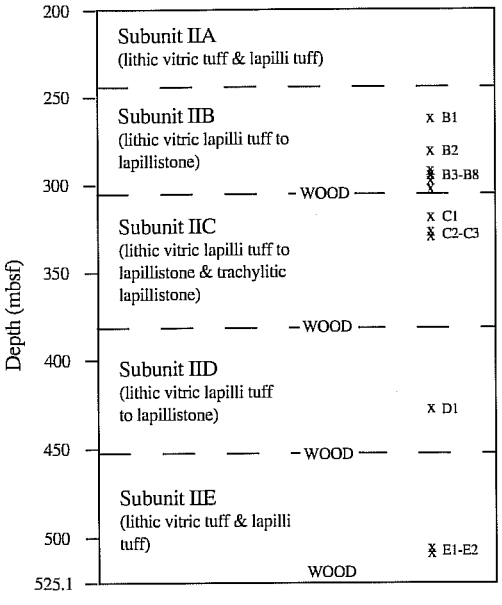

Fig. 2. Stratigraphic section of core recovered from Hole 1184A showing location of samples and of wood-bearing horizons. Modified from Mahoney *et al.* (2001) and White *et al.* (2004).

Samples and experimental methods

Samples

The drilling at Site 1184 recovered an upper interval of calcareous ooze (Unit I) and more than 330 m of volcaniclastic rocks (Unit II) (Fig. 2). Unit II is divided into six subunits (A, B, C, D, E and F) on the basis of changes in grain size, lithology and sedimentary structures (Thordarson 2004). Common lithologies include tuff, lapilli tuff and lapillistone, all of which contain occasional lithic clasts. The lithic clasts are primarily basalt, diabase or re-worked volcaniclastic material. The near absence of large lapilli suggests that the volcaniclastic material was deposited some distance from the volcanic centre (Mahoney *et al.* 2001). For the most part, the rocks recovered from Site 1184 are moderately to highly altered, although some unaltered glass is present below Core 38R. Small oxidized red lapilli are present, especially in Subunit IIC, and, as noted above, wood fragments are present at the boundaries between subunits IIB–C, IIC–D, IID–E, and IIE–F. A thinly bedded, fine-grained tuff in subunit IIC appears to be a primary ash-fall deposit (Mahoney *et al.* 2001). These features indicate emergence of the OJP in this region.

A total of 14 basaltic clasts extracted from subunits IIB, IIC, IID and IIE were selected for this study (Fig. 2). In hand sample the clasts were non-vesicular to sparsely vesicular and aphyric to sparsely plagioclase-phyric basalts. The clasts were generally small (1–4 cm) and were a greyish colour. We refer to these as Clasts B1–E2, with the letter referring to the subunit and the number referring to the position within the subunit. For example, Clast B2 is higher in the core than clast B7 (see Tables 1 and 2 for core intervals).

Analytical methods

The basalt clasts were cut from the volcaniclastic matrix using a water-cooled rock saw, then ground on a diamond grinding wheel in order to remove any excess adhering matrix and to remove any contamination from the rock saw. The biggest clasts were broken into <0.5 cm chips that were crushed further in an alumina SPEX jaw crusher. The jaw crusher was thoroughly cleaned with ultrapure water and a clean nylon scouring pad between the processing of different clasts. The chips were washed in 18 MΩ water for 30 min in an ultrasonic bath. They were then air dried and examined using a binocular microscope. Although all samples displayed varying degrees of alteration, chips exhibiting excessive alteration were removed. The chips were powdered using a SPEX Mixer/Mill in alumina shaker bombs or by hand in an agate mortar and pestle (depending upon the amount of sample available).

Major-element concentrations were determined via inductively coupled plasma-optical emission spectroscopy (ICP-OES) at the University of Notre Dame. Approximately 0.1 g of sample powder was mixed with 0.5 g of lithium metaborate and fused at 1025°C for 30 min The molten pellets were quenched in 5% HNO_3, which was transferred to polypropylene bottles and made up to 100 g with 5% HNO_3. This solution was placed in an ultrasonic bath for 1 h in order to facilitate complete dissolution of the fused glass. The geochemical reference materials analysed for major elements during this study were BHVO-2, BIR-1 and BPL-1. Drift was monitored by running a standard solution every four analyses. Calibration was performed by taking blank- and drift-corrected counts of a selected reference material and dividing by the accepted elemental concentrations. This allowed for a simple data reduction algorithm similar to the procedure used for shipboard ICP-OES reduction during Leg 192 (Mahoney *et al.* 2001). Between each sample solution, 5% nitric

acid was used to remove any memory effects by flushing any remaining solution from the tubing and glassware. Blank levels were generally very low (e.g., the average raw counts per second (cps) of Ti (λ = 334.94) for blanks were 890 v. 3 768 000 cps for BHVO-2) indicating that the 5% nitric acid flush was efficient in minimizing memory effects. Standard deviations for replicate reference materials were generally less than 6%, although for K_2O and Na_2O the standard deviation could be as high as 25% due to a combination of low abundance, poor sensitivity and high background. Loss on ignition (LOI) was determined by heating between 0.1 and 0.5 g of sample powder in platinum crucibles at 1025°C for 4 h. The samples were weighed before and after removal from the oven, and total weight per cent LOI was determined.

Trace-element abundances were quantified via ICP-mass spectrometry (ICP-MS) at the University of Notre Dame (see Neal 2001 for full analytical details). If it appeared that immobile element ratios (i.e. Zr/Hf, Zr/Nb, Nb/Ta, Nb/La and Zr/Sm) deviated from typical OJP basalt ranges (Tejada *et al.* 1996, 2002; Neal *et al.* 1997), an aliquot of the sample powder was fused using sodium peroxide as a flux to ensure complete dissolution of any refractory phases (Longerich *et al.* 1990). BHVO-1 was used as the reference material for the trace-element analyses. Blank levels were below 100 cps, and standard deviations (SDs) for replicated standard reference materials were generally less than 3% (V and Cr >10%, Ni and Zn between 5 and 10%, all others below 3%).

Strontium-, Nd- and Pb-isotopic measurements were made on five basaltic clasts using a Micromass Sector 54 multi-collector thermal ionization mass spectrometer at the Scripps Institution of Oceanography (SIO). In order to minimize the effects of sea-water alteration on the Sr and Nd isotopic composition, the sample powders were subjected to a harsh multi-step leaching procedure similar to that described by Mahoney (1987) and Castillo *et al.* (1991). Unleached powders were used for Pb-isotope analysis because almost all the leached powders yielded very low concentrations of Pb, indicating that most of the Pb was in leachable phases. Both the leached and unleached powders were dissolved in clean Teflon vessels using *c.* 1 ml of a 2:1 mixture of concentrated HF and HNO_3, and heated on a hotplate at low power for 16–24 h. The resulting solutions were evaporated to dryness, redissolved in a small amount of concentrated HNO_3, evaporated to dryness and the procedure repeated. Strontium and rare earth elements (REE) were first separated in primary cation-exchange columns; Nd was separated from the rest of the REE by passing the REE aliquots through small EDTA ion-exchange columns. Lead was separated using a standard anion-exchange method (e.g. Lugmair & Galer 1992; Janney & Castillo 1996) in a HBr–HNO_3 medium. Concentrations of Rb, Sr, Sm, Nd, U, Th and Pb were measured on separate dissolutions using a high-resolution ICP-MS at SIO using a procedure similar to that described by Janney & Castillo (1996).

Results

Petrography

The generally small size of the clasts (sometimes <1 cm after grinding) meant that thin sections could only be made for nine of the 14 samples, but at least one thin section was made of clasts from each Site 1184 subunit. Plagioclase and clinopyroxene are the most common groundmass phases in these samples and vary from extremely fine-grained crystals (<0.05 mm) to larger crystals (up to about 0.3 mm) with a sub-ophitic–intergranular texture. In one of the most altered samples (Clast C1, LOI = 10.38 wt%), secondary zeolite is extremely abundant (identified as natrolite based on this sample having Na_2O = 5.73 wt%). A trachytic texture is still evident (Fig. 3a). Even in samples with relatively low LOI (e.g. Clast B6, LOI = 4.88 wt%), clinopyroxene is generally altered and replaced by clays (Fig. 3b). In samples with larger grain sizes (e.g. Clast E1), clinopyroxene is generally partially altered and replaced by brown clays, but the plagioclase crystals are generally unaltered (Fig. 3c). In Clasts C1, B3, B8, E1 and E2, zeolite minerals are present as vesicle fill and veins in the surrounding matrix.

Major elements

Major-element concentrations and LOI of the 14 basalt clasts analysed by ICP-OES are presented in Table 1. These data have been recalculated on a volatile-free basis. The uncorrected major element totals vary from 97.0 to 106.8 wt%. The large range of major-element totals is controlled by two samples: the consistent low totals of sample C2 (replicated multiple times on different fusions) and the high total of sample D1, for which sample powder was extremely limited and thereby precluded multiple fusions. We suggest that these data be treated with caution. The altered nature of all Site 1184 clasts samples is highlighted by the fact that the majority of samples have at least 5 wt% LOI (the total range is 1.6–11 wt%). Concentrations of CaO,

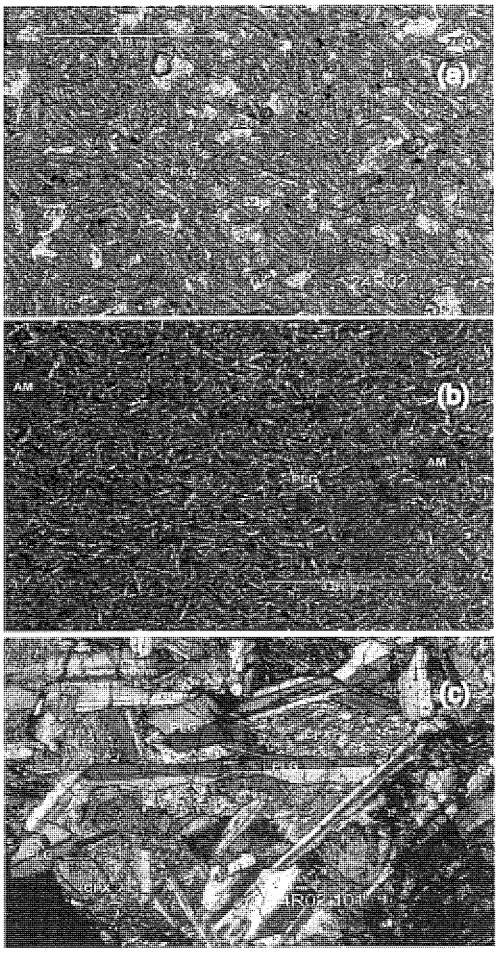

Fig. 3. Photomicrographs of basalt clasts. (**a**) Group 4 clast C1 (sample 24R-2, 68–70 cm) in plane-polarized light showing clear zeolite (probably natrolite) and small plagioclase laths. (**b**) Group 1 clast B6 (sample 21R-6, 73–77 cm) in plane-polarized light showing clinopyroxene altered to a brown mineral; small plagioclase laths define a subtrachytic texture. (**c**) Group 1 clast E1 (sample 44R-2, 101–105 cm) under crossed polars. This sample has one of the lowest LOI values in the Site 1184 suite, yet clinopyroxene still shows signs of alteration. Mineral abbreviations are as follows: ZEO, zeolite; PLG, plagioclase; CPX, clinopyroxene; and AM, alteration mineral.

SiO_2 and MgO are negatively correlated with LOI (CaO shows the best correlation as seen in Fig. 4a), and K_2O exhibits a positive correlation (Fig. 4b; Na_2O displays a poor positive correlation with LOI). In terms of the SiO_2 v. total alkalis classification diagram (Fig. 5a), these samples are transitional between alkalic and tholeiitic. However, as indicated in Figure 4b, alteration has variably increased Na_2O and K_2O levels. Fresh glass clasts analysed by White *et al.* (2004) plot as low-K tholeiites. When elements considered to be immobile under low-temperature alteration conditions are used to discriminate between alkali and tholeiitic basalts, the basalt clasts plot strictly in the tholeiitic field (Fig. 5b).

Trace elements

Considerable variability in trace-element abundances (Table 2, re-calculated to a volatile-free basis) and in element/element ratios, especially for ratios of normally immobile elements (e.g. Nb/La), is displayed by the Site 1184 basalt clasts. We have subdivided our basalt clasts into four groups on the basis of incompatible-element profiles (Fig. 6a–d). Group 1 comprises four clasts (Clasts B1, B6, E1 and E2; Fig. 6a) that have primitive-mantle-normalized profiles similar to those of the Kwaimbaita Formation lavas. These clasts also possess among the lowest LOI values of all clasts analysed in this study (1.68–4.88 wt%; Table 1). Group 2 clast compositions (Clasts B2, B3, B4, B8 and D1; Fig. 6b) show greater variability, although the heavy REE (HREE) have similar normalized abundances to those of lavas from the Kwaimbaita Formation. These clasts exhibit higher LOI values (4.01–7.85 wt%). Clast D1 exhibits a deep Zr–Hf trough and light REE (LREE) enrichment (Fig. 6b). This could reflect the incomplete dissolution of a refractory oxide or other phase, possibly zircon, during sample preparation; however, the HREE are not depleted relative to the Kwaimbaita Formation lava compositions (Fig. 6b). The extremely limited amount of basalt clast from this sample precluded multiple dissolutions (i.e. flux fusion), so the veracity of this anomaly cannot be assessed and, thus, must be interpreted with caution. However, in other aspects the sample is similar to the Kwaimbaita Formation basalts (i.e. HREE, Nb and Ta abundances). Group 3 clasts (Clasts B5 and B7; Fig. 6c) have normalized profiles similar to those of Kroenke-type basalts (Sites 1185 and 1187; Fitton & Godard 2004), although in Clast B5 there are depletions at Nb–Ta and Zr–Hf relative to the REE. These profiles have been duplicated by separate dissolution, including the sodium peroxide fusion method (Longerich *et al.* 1990). These two clasts also contain the highest Ni abundances of the 14 clasts analysed in this study (222–296 ppm; the range of Ni abundance reported from the Kroenke-type basalts is 170–230 ppm – Fitton & Godard 2004). Clast B5 also has TiO_2 abundances comparable to those

Table 1. *Major element concentrations* (wt%), loss on ignition, and core intervals for ODP Site 1184 basaltic clasts*

Core, Interval (cm)	Clast	Group	Depth (mbsf)	SiO_2	TiO_2	Al_2O_3	$Fe_2O_3^T$	MnO	MgO	CaO	Na_2O	K_2O	P_2O_5	Total†	LOI
18R-2, 102–104	B1	1	260.96	49.60	1.24	12.21	13.08	0.26	8.94	9.73	4.44	0.34	0.17	99.4	4.25
20R-4, 50–52	B2	2	282.89	51.62	1.01	14.45	7.81	0.14	7.09	13.29	3.90	0.61	0.08	99.2	6.22
21R-5, 40–47	B3	2	293.08	51.15	1.40	15.94	10.91	0.04	4.40	4.60	3.16	8.25	0.16	100.4	7.32
21R-5, 55–60	B4	2	293.23	47.19	1.26	18.59	18.69	0.10	10.62	0.85	1.75	0.81	0.14	99.2	7.85
21R-6, 28–30	B5	3	294.46	53.45	0.73	17.00	7.74	0.11	5.47	12.64	2.46	0.33	0.08	98.6	3.96
21R-6, 73–77	B6	1	294.91	49.89	1.02	14.58	11.39	0.30	8.24	9.93	4.06	0.56	0.03	100.0	4.88
22R-1, 24–27	B7	3	297.54	50.81	1.02	15.34	10.28	0.28	8.11	8.63	4.46	1.05	0.03	103.1	6.87
22R-4, 120–123	B8	2	301.77	52.41	1.01	13.83	7.16	0.16	7.75	13.36	3.37	0.75	0.21	97.3	4.01
24R-2, 68–70	C1	4	318.03	48.52	1.05	17.14	12.70	0.28	7.07	4.83	5.73	2.00	0.67	103.8	10.38
25R-5, 16–18	C2	4	330.85	49.93	2.12	13.00	18.02	0.39	6.44	5.26	3.38	1.10	0.37	97.0	7.22
25R-6, 115–117	C3	4	333.10	50.07	1.97	15.23	14.99	0.39	5.11	6.49	4.53	0.91	0.33	99.1	11.83
35R-8, 32–35	D1	2	432.30	49.49	1.18	12.83	12.99	0.18	7.60	9.88	5.22	0.56	0.07	106.8	4.87
44R-2, 101–105	E1	1	511.68	49.27	0.95	13.37	11.13	0.21	7.90	13.93	2.95	0.26	0.04	100.0	3.17
44R-2, 126–132	E2	1	512.43	48.86	0.97	13.97	11.51	0.19	7.89	13.31	2.99	0.27	0.03	100.3	1.68
‡BHVO-2 average				50.0	2.71	13.7	12.3	0.18	7.24	11.4	2.21	0.52	0.29		
Recommended values				49.9	2.73	13.5	12.3	0.13	7.23	11.4	2.22	0.52	0.27		
S.D (1σ) ($n = 7$)				1.5	0.07	0.5	0.2	0.01	0.09	0.3	0.12	0.07	0.04		
BIR-1 average ($n = 2$)				50.2	1.02	16.2	12.1	0.22	9.89	14.3	2.34	bd	0.07		
Recommended values				47.96	0.96	15.5	11.3	0.18	9.70	13.3	1.82	0.03	0.021		
BPL-1 average ($n = 2$)				50.8	2.49	16.8	14.1	0.24	8.43	10.6	2.85	0.30	0.72		
Recommended values				46.1	2.30	14.8	13.6	0.18	8.12	9.7	2.31	1.11	0.49		

* all major- and trace-element data presented have been normalized to 100% on a volatile-free basis.
mbsf, metres below seafloor; LOI, loss on ignition; bd, below detection limit.
Total† is the un-normalized major-element total of each clast + LOI.
‡ BHVO-2 recommended values from USGS preliminary certificate of analysis. BPL-1 recommended values from Scott Hughes, Idaho State University, pers. comm. BIR-1 values from Flanagan (1984) and Gladney & Roelandts (1988).

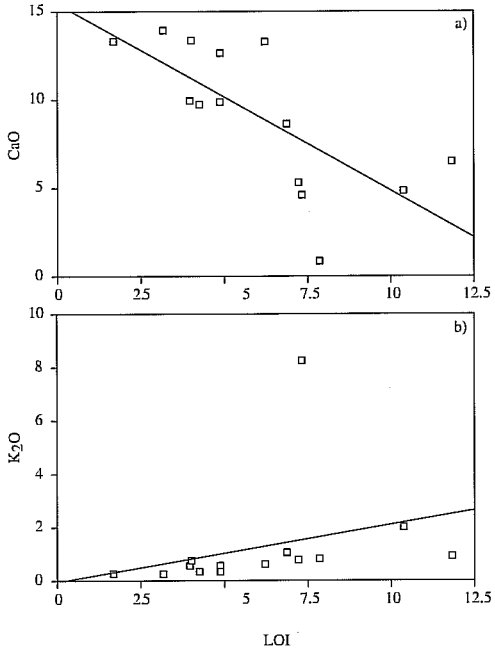

Fig. 4. (**a**) Loss on ignition (LOI) v. CaO (wt%) and (**b**) LOI v. K_2O (wt%) indicating that major elements can be mobilized and either lost (CaO) or gained (K_2O) during sea-water alteration of basalts.

of Kroenke-type basalts (TiO_2 = 0.73 wt%, v. 0.733 wt% in average Kroenke-type basalt), but has lower overall Zr and Nb contents (24.2 and 1.36 ppm, respectively, v. 40.6 and 2.18 ppm in average Kroenke-type basalt). Clast B7 contains higher Zr (56.8 ppm), Nb (2.95 ppm) and TiO_2 (1.02 wt%) abundances, and appears to be intermediate between the Kroenke-type and Kwaimbaita-type compositions. Group 4 clast compositions (Clasts C1, C2 and C3) have more enriched incompatible-element concentrations (specifically, Nb, Ta, Th and the HREE) than average Wairahito basalts (the most evolved rock type so far found on the OJP) described by Birkhold (2000) from the island of Makira (also known as San Cristobal) (Fig. 6d). Clasts C1 and C3 exhibit negative Sr and Eu anomalies that are consistent with plagioclase fractionation. In addition, the trace-element composition of the volcaniclastic matrix within which the three Group 4 clasts were contained also shows increased levels of Nb, Ta and Th over the REE (Fitton & Godard 2004). However, the Nb, Ta, Th or REE abundances of the matrix are not as enriched as in the Group 4 clasts.

Clasts B2, B5, B8, E1 and E2 all exhibit a curious positive Y anomaly of varying magnitude, which has been replicated twice using separate dissolutions, including sodium peroxide fusion. Such an anomaly is not seen in lavas typical of the Kwaimbaita-type lavas.

Fractionation of the LREE from high field strength elements (HFSE), such as Nb, is seen in Clasts B2, B3, B4, B8, C1, C2 and C3 (Fig. 6b, d). Clast B8 is Kwaimbaita-like over most of the profile and in certain incompatible-element ratios (La/Lu = 9.6 v. 10.5 for average Kwaimbaita-type basalt, La/Ce = 0.32 v. 0.34), yet has a $(Nb/La)_{PM}$ ratio of 1.7 (v. 1.09 for average Kwaimbaita-type basalt). As with the positive Y anomaly, this type of fractionation is not seen in typical Kwaimbaita Formation basalts (Tejada *et al.* 1996, 2002; Neal *et al.* 1997).

Radiogenic isotope ratios

Four samples (Clasts B4, B7, C3 and E1) were analysed for Sr-, Nd- and Pb-isotope ratios, and Clast B8 for Sr- and Nd-isotope ratios (Table 3). The five clasts analysed represent at least one sample from each of the groups defined on the basis of incompatible elements. All isotope data were age-corrected to 120 Ma (Chambers *et al.* 2004) using high-resolution ICP-MS parent–daughter data obtained from splits of the solutions analysed for isotopes, except for U and Th values of Clast B4, which were determined by high-resolution ICP-MS on leached powders. Age-corrected ε_{Nd} values ($\varepsilon_{Nd(t)}$) form a narrow range (+6.0–+6.5), whereas initial $^{87}Sr/^{86}Sr$ ($^{87}Sr/^{86}Sr_I$) and age-corrected $^{206}Pb/^{204}Pb$ ($^{206}Pb/^{204}Pb_{(t)}$) exhibit relatively more variation (0.70288–0.70480 and 18.139–18.458, respectively; Table 3). The range of $\varepsilon_{Nd(t)}$ is within that for the Kwaimbaita basalts (Fig. 7a, b). Although the wide range of Sr- and Pb-isotope compositions overlaps with the ranges for the Kwaimbaita and the Singgalo basalts (cf. Tejada *et al.* 2002) (Fig. 7a, b), we interpret the range in our data to be a result of secondary alteration effects (see later for further discussion). Therefore, we shall not use our Sr- and Pb-isotopic results in the following petrogenetic interpretation.

Discussion

The influence of alteration

The basalt clasts from Site 1184 are lithic fragments derived from coeval or possibly pre-existing volcanic rocks during explosive phreatomagmatic eruptions (Thordarson 2004). Therefore, alteration effects are a major concern

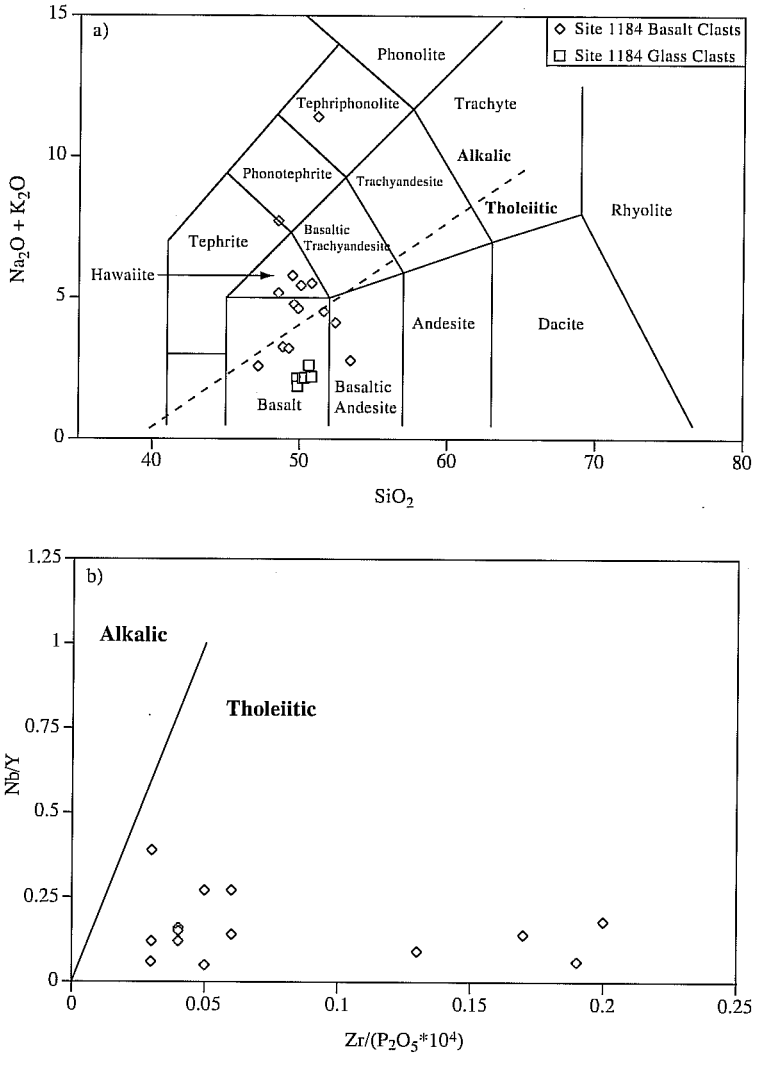

Fig. 5. Classification of the basaltic clasts. (**a**) SiO_2 v. total alkalis ($Na_2O + K_2O$), where the dashed line separates Hawaiian tholeiitic and alkali lavas (Macdonald & Katsura 1964). Data for Site 1184 glass clasts are from White *et al.* (2004). Fields of rock types are from Le Bas *et al.* (1986). (b) Nb/Y v. $Zr/(P_2O_5 \times 10^4)$ after Winchester & Floyd (1976). The Site 1184 clasts plot as transitional between alkalic and tholeiitic on the SiO_2 v. total alkali plot, yet strongly tholeiitic on the Nb/Y v. $Zr/(P_2O_5 \times 10^4)$ plot, suggesting that Na_2O and K_2O were increased during alteration of these samples.

in our study and here we evaluate these prior to any petrogenetic interpretation.

The variability of the major-element composition of the clasts relative to the OJP basalt groups is interpreted primarily to be the result of alteration. The generally high LOI values, coupled with petrographic observations, demonstrate the moderately to highly altered nature of these clasts. In Figure 4a, b it is seen that CaO is negatively correlated and K_2O is positively correlated with LOI, demonstrating that elements can be depleted or enriched (respectively) during alteration. Indeed, many studies in the last several decades (e.g. Hart 1970) have reported that during low-temperature submarine alteration, ocean-ridge tholeiites lose SiO_2, CaO, and MgO, and gain K_2O, some Fe_2O_3, MnO, Na_2O, and P_2O_5. It would appear that the Site 1184 clasts have only gained K_2O (and possibly Na_2O) and lost CaO, SiO_2 and

Table 2. *Trace-element concentrations* of Leg 192, Site 1184 basaltic clasts (all values are in ppm)*

Core	18R-2	20R-4	21R-5	21R-5	21R-6	21R-6	22R-1	22R-4	24R-2	25R-5	25R-6	35R-8	44R-2	44R-2	24R-2	25R-5	25R-6	BHVO-2‡	SD	Recommended
Interval (cm)	102–104	50–52	40–47	55–60	28–30	73–77	24–27	120–123	68–70	16–18	115–117	32–35	101–105	126–132	68–70	16–18	115–117	$n = 7$		values§
Clast	B1	B2	B3	B4	B5	B6	B7	B8	C1	C2	C3	D1	E1	E2	MC1†	MC2†	MC3†			
Group	1	2	2	2	3	1	3	2	4	4	4	2	1	1						
Li	9.09	3.69	7.06	10.5	bd	3.74	1.28	2.97	8.74	5.51	6.29	2.59	5.71	2.49	8.78	9.38	10.8	4.7	0.7	5
Be	0.16	0.15	0.08	0.11	0.23	0.26	1.16	0.12	0.20	0.23	0.28	0.31	0.20	0.25	0.49	0.52	0.54	1.05	0.1	*1.1*
Sc	66.6	39.3	41.9	56.1	74.6	52.8	221.9	48.0	17.7	37.8	42.8	48.9	46.2	45.4	49.7	51.8	53.6	33.1	3.0	32
V	568.4	192.7	522.5	771.1	1259	375.9	1785	410.3	179.8	183.2	192.6	482.1	296.6	285.5	217.0	235.8	238.5	336.3	14.9	317
Cr	646.8	298.5	177.7	243.5	337.3	378.1	946.4	210.8	13.7	15.4	33.4	273.9	325.6	362.7	177.1	194.8	192.6	284.7	48.8	280
Co	55.5	25.4	97.5	45.0	58.7	51.2	181.0	32.9	24.7	38.8	38.3	57.2	51.0	54.3	50.3	50.9	54.2	52.3	4.3	45
Ni	107.2	71.2	88.9	88.5	234.3	89.4	307.7	70.9	14.3	12.3	17.5	110.5	111.9	116.5	68.3	75.6	74.1	127.6	7.9	119
Cu	74.7	9.24	406.8	27949	232.9	169.5	804.6	51.8	49.3	61.9	69.2	49.7	153.1	162.0	138.1	144.9	146.4	139.0	2.2	127
Zn	211.3	24.0	17.9	45.6	23.3	139.5	632.2	43.3	123.4	192.0	198.7	73.2	140.8	93.6	151.3	148.1	167.0	111.0	5.4	103
Ga	18.8	16.2	15.1	26.9	23.1	20.4	81.1	16.6	32.1	24.7	18.9	19.2	17.9	18.8	35.1	24.0	34.4	23.3	1.4	*21*
Rb	4.57	2.03	16.5	12.9	1.76	1.85	5.06	2.40	5.50	12.0	7.87	0.21	0.27	0.33	10.8	9.36	11.2	9.7	1.5	9.8
Sr	82.7	105.1	49.9	31.7	369.1	96.0	92.8	123.4	148.7	89.8	222.7	88.2	102.0	96.3	145.5	117.7	189.2	399.0	22.8	389
Y	21.8	44.3	30.7	28.0	21.0	22.3	16.1	55.5	45.5	56.6	54.3	23.5	30.5	46.5	39.3	38.0	36.7	26.0	1.9	26
Zr	66.3	42.9	57.9	85.5	24.2	56.8	56.8	59.9	212.2	181.1	187.6	28.1	52.7	53.7	90.1	89.2	86.1	172.1	15.4	172
Nb	3.50	2.24	3.66	4.00	1.36	3.21	2.95	6.56	17.5	15.1	14.7	3.51	2.60	2.96	8.78	7.40	8.41	19.8	1.0	18
Ba	7.65	28.9	157.7	54.1	14.2	26.4	39.7	40.7	19.1	46.5	47.5	8.17	9.29	9.55	32.1	36.4	127.7	138.9	3.3	130
La	3.22	1.67	1.98	8.4	1.92	3.12	2.89	3.83	7.59	7.11	7.39	4.01	2.78	2.85	7.35	7.88	7.40	16.3	0.4	15
Ce	9.03	6.88	5.25	17.5	5.96	9.12	7.48	12.1	24.2	21.1	21.2	13.6	7.81	8.37	18.3	18.4	17.7	40.4	1.7	38
Pr	1.51	1.30	0.86	2.3	1.05	1.45	1.14	2.1	3.68	3.38	3.28	2.07	1.29	1.34	2.70	2.70	2.59	5.9	0.1	*5.7*
Nd	7.16	7.09	4.21	10.6	5.05	6.91	5.75	10.1	16.8	16.3	15.3	8.98	6.46	6.30	11.7	11.6	11.1	25.1	0.5	25
Sm	2.66	2.70	1.76	3.22	1.67	2.50	1.90	3.08	5.87	5.72	5.56	2.92	2.15	2.42	3.55	3.46	3.37	6.6	0.5	6.2
Eu	0.80	0.81	0.67	0.74	0.59	0.87	0.69	1.01	1.54	1.59	1.55	1.08	0.82	0.84	1.39	1.29	1.28	2.19	0.1	*2.06*
Gd	3.57	3.63	3.23	4.13	2.46	3.32	2.69	4.32	7.41	8.27	7.67	3.63	3.09	3.24	5.24	4.98	4.79	6.75	0.1	6.3
Tb	0.62	0.63	0.67	0.72	0.42	0.61	0.45	0.72	1.31	1.48	1.42	0.64	0.55	0.56	0.88	0.89	0.83	1.01	0.05	0.9
Dy	4.13	4.17	4.71	4.83	2.54	4.21	2.97	4.49	8.44	10.3	9.64	4.27	3.59	3.84	6.17	6.01	5.63	5.68	0.26	*5.2*
Ho	0.85	0.88	1.10	1.05	0.55	0.92	0.59	1.00	1.77	2.21	2.14	0.88	0.80	0.80	1.38	1.34	1.27	1.04	0.04	1.0
Er	2.45	2.58	3.45	3.31	1.65	2.66	1.69	2.92	4.93	6.81	6.44	2.50	2.28	2.36	4.22	4.11	3.87	2.77	0.12	*2.4*
Tm	0.37	0.38	0.56	0.50	0.25	0.39	0.25	0.43	0.75	0.99	1.00	0.37	0.35	0.36	0.64	0.63	0.58	0.38	0.03	*0.33*
Yb	2.57	2.55	3.44	3.38	1.40	2.62	1.62	2.65	5.29	7.53	6.74	2.25	2.25	2.45	4.06	4.04	3.80	2.15	0.1	2.0
Lu	0.33	0.34	0.53	0.51	0.22	0.39	0.21	0.40	0.75	1.06	0.97	0.31	0.32	0.33	0.60	0.59	0.56	0.29	0.02	0.28
Hf	1.79	1.54	1.80	2.45	0.75	1.65	1.56	1.36	5.31	5.01	4.65	0.99	1.55	1.51	2.41	2.39	2.25	4.48	0.12	4.1
Ta	0.21	0.25	0.25	0.23	0.08	0.21	0.16	0.20	1.13	0.89	0.91	0.22	0.16	0.18	0.46	0.42	0.42	1.30	0.1	1.4
Pb	0.38	0.14	0.06	0.04	bd	bd	bd	bd	0.64	0.32	0.31	0.06	0.08	0.05	0.76	0.90	0.71	1.54	0.07	*2.05*
Th	0.27	0.22	0.27	0.33	0.07	0.24	0.14	0.60	1.78	1.61	1.50	0.18	0.22	0.24	0.65	0.60	0.57	1.30	0.1	1.20
U	0.05	0.01	0.09	0.13	0.05	0.08	0.04	0.01	0.06	0.11	0.34	0.10	0.09	0.05	0.11	0.12	0.13	0.47	0.04	*0.42*

* All trace-element data have been normalized on a volatile-free basis.
† Concentrations of samples MC1–MC3 are of the volcaniclastic matrix surrounding clasts C1–C3, respectively. Clast names are composed of the subunit from which the clast was extracted and relative position within core (see text).
‡ BHVO-2 recommended values from USGS preliminary certificate of analysis (Wilson 1997).
§ Recommended values in italics are for BHVO-1 (Govindaraju 1994).
bd, below detection limit.

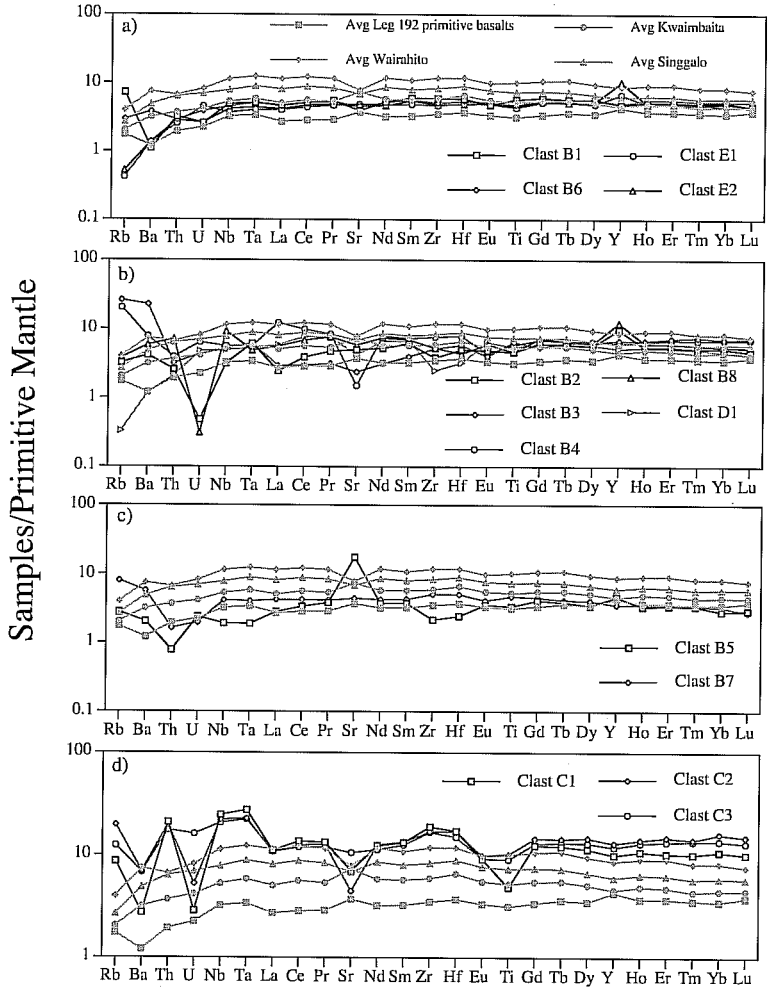

Fig. 6. Primitive-mantle-normalized incompatible-element plots of (**a**) Group 1 – Clasts B1, B6, E1 and E2; (**b**) Group 2 – Clasts B2, B3, B4, B8 and D1; (**c**) Group 3 – Clasts B5 and B7; and (**d**) Group 4 – Clasts C1, C2 and C3. The grey profiles represent Kwaimbaita-type basalt (circle), Singgalo-type basalt (triangle), Kroenke-type basalt (square) and the Wairahito Formation basalts (diamond). Group 1 clasts show similar profiles to Kwaimbaita-type basalt, Group 3 clasts show affinity to Kroenke-type basalt and Group 4 clasts are distinct from the main basalt types. Group 2 clasts exhibit more compositional variability, which is probably due to more intense alteration, although they have HREE profiles similar to Kwaimbaita-type basalt. See text for details. Data from which average OJP basalt compositions were calculated are from Neal *et al.* (1997), Tejada *et al.* (1996, 2002), Birkhold (2000) and Mahoney *et al.* (2001).

MgO to any significant degree, although the Group 4 samples with >5 wt% LOI have the highest P_2O_5 contents.

In terms of incompatible trace elements, and Sr- and Pb-isotope ratios, the basalt clasts from Site 1184 exhibit much more variation than do basalt compositions across the OJP (e.g. Fig. 7a–c). This is also probably a result of sea-water alteration, which affected the abundances of fluid-mobile trace elements such as Rb, Sr, Pb and, to a certain extent, U (e.g. Hart *et al.* 1974; Menzies & Seyfried 1979). The effect of sea-water alteration on both trace elements and isotopes is demonstrated by the negative correlation between bulk-clast Sr concentrations and isotopic compositions (measured on leached splits of sample) (Fig. 8). The negative correlation suggests that the clasts with low Sr

Table 3. *Sr-, Nd- and Pb-isotopic data for basaltic clasts from ODP Site 1184*

Core	21R-5	22R-1	22R-4	25R-6	25R-6 Dupl.	44R-2	44R-2 Dupl.
Interval (cm)	55–60	24–27	120–123	115–117	115–117	101–105	101–105
Clast	B4	B7	B8	C3	C3	E1	E1
Group	2	3	2	4	4	1	1
Rb	18.2	5.86	1.07	2.20		0.09	
Sr	43.3	113.7	110.2	18.5		64.4	
$^{87}Sr/^{86}Sr$	0.706850	0.703944	0.704852	0.703467		0.703654	
$^{87}Sr/^{86}Sr_{(t)}$	0.704779	0.703690	0.704804	0.702881		0.703647	
Sm	0.9	0.48	3.68	3.13		1.27	
Nd	3.51	1.18	11.1	6.03		2.74	
$^{143}Nd/^{144}Nd$	0.512924	0.513002	0.512976	0.513042		0.513012	
$^{143}Nd/^{144}Nd_{(t)}$	0.512803	0.512810	0.512819	0.512797		0.512793	
$\varepsilon Nd_{(t)}$	6.2	6.3	6.5	6.1		6.0	
Th	0.18	0.31		1.20		0.30	
U	0.35	0.06		0.23		0.06	
Pb	0.48	0.19		0.30		0.36	
$^{206}Pb/^{204}Pb$	19.101±8	18.831±7		19.053±3	19.037±6	18.567±2	18.566±6
$^{207}Pb/^{204}Pb$	15.541±7	15.543±6		15.577±2	15.556±5	15.519±1	15.516±6
$^{208}Pb/^{204}Pb$	38.763±17	38.614±15		39.000±6	38.941±13	38.380±4	38.366±14
$^{206}Pb/^{204}Pb_{(t)}$	18.144	18.458		18.139	18.124	18.371	18.370
$^{207}Pb/^{204}Pb_{(t)}$	15.499	15.525		15.532	15.511	15.509	15.506
$^{208}Pb/^{204}Pb_{(t)}$	38.059	38.059		37.437	37.380	38.060	38.046

Rb, Sr, Sm, Nd, Th, U and Pb concentrations (ppm) from analysis of leached powder. Age (t) is taken as 120 Ma. Duplicate analyses were made on different dissolutions of the same unleached power. Analytical uncertainty for $^{87}Sr/^{86}Sr$ measurements is ±0.000018 but in-run precisions were better than ±0.000012. Sr-isotopic ratios were measured by dynamic multi-collection, fractionation-corrected to $^{86}Sr/^{87}Sr = 0.1194$ and normalized to $^{87}Sr/^{86}Sr = 0.71025$ for NBS 987. Analytical uncertainty for $^{143}Nd/^{144}Nd$ measurements is 0.000014 (0.3 ε units) but in-run precisions were better than 0.000010. Nd-isotopic ratios were measured in oxide form by dynamic multi-collection, fractionation-corrected to $^{146}NdO/^{144}NdO = 0.72225$ ($^{146}Nd/^{144}Nd = 0.7219$) and are reported relative to $^{143}Nd/^{144}Nd = 0.511850$ for the La Jolla Standard. Pb-isotopic ratios were measured by static multi-collection and are reported relative to the values of Todt *et al.* (1996) for NBS SRM 981; the long-term errors measured for this standard are ±0.008 for $^{206}Pb/^{204}Pb$ and $^{207}Pb/^{204}Pb$, and ±0.024 for $^{208}Pb/^{204}Pb$. The within-run errors shown refer to the last significant figure. Estimated uncertainties on concentrations are *c.*1% for both Sm and Nd, and *c.*2% on Rb, Sr, U, Th and Pb. Total procedural blanks are negligible: <10 picograms (pg) for Nd, <35 pg for Sr, <3 pg for Th, <5 pg for U and <60 pg for Pb. $\varepsilon_{Nd} = 0$ today corresponds to $^{143}Nd/^{144}Nd = 0.51264$; for $^{147}Sm/^{144}Nd = 0.1967$, $\varepsilon_{Nd(t)} = 0$ corresponds to $^{143}Nd/^{144}Nd = 0.512486$ at 120 Ma.

contents and high $^{87}Sr/^{86}Sr$ ratios have exchanged significant amounts of Sr with sea-water (8 ppm Sr, present day $^{87}Sr/^{86}Sr = 0.709$, at 120 Ma $^{87}Sr/^{86}Sr$ = *c.* 0.707 – Hess *et al.* 1986; DePaolo & Ingram 1985). The clasts with high $^{87}Sr/^{86}Sr$ have similar Sr-isotopic compositions to sea water at 120 Ma, indicating that most of alteration occurred during or soon after the eruptions. As noted earlier, the Pb-isotopic signature appears to have been affected by alteration. White *et al.* (2004) observed that, in the bulk volcaniclastic rocks at Site 1184, Sr- and Pb-isotope ratios have been affected by sea-water alteration. The same type of result was also seen in the Singgalo-type vitric tuff at Site 1183 (Tejada *et al.* 2004).

A number of studies have shown that the concentrations of some trace elements, such as REE and HFSE, in igneous rocks are generally not affected during mild sea-water alteration (e.g. Ludden & Thompson 1979; Bienvenu *et al.* 1990). Yet, it has also been documented that the REE are relatively mobile during more extensive alteration compared to the HFSE, and that the LREE are preferentially mobilized over the HREE (Ludden & Thompson 1979; Bach & Irber 1998; Kikawada *et al.* 2001). Overall, the Site 1184 basalt clasts exhibit large variations in element ratios such as La/Nb, La/Ta, Th/Ta, Th/Nb and Zr/Hf. Kurtz *et al.* (2000) reported enrichments in alteration-resistant, insoluble trace elements (Zr, Nb, Hf, Ta, Th) in strongly weathered Hawaiian soils over parent lava values due to extensive mass loss of more soluble major elements during soil formation. The presence of wood and oxidized horizons

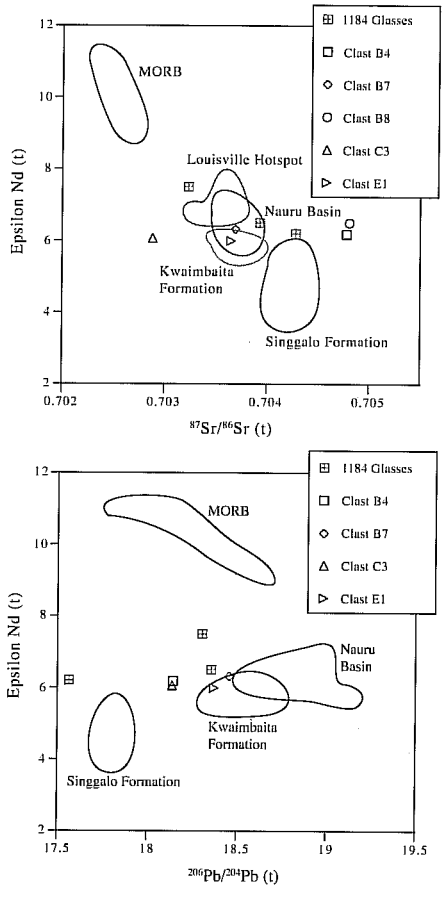

Fig. 7. (**a**) $^{87}Sr/^{86}Sr_{(t)}$ v. $\varepsilon_{Nd(t)}$; (**b**) $^{206}Pb/^{204}Pb_{(t)}$ v. $\varepsilon_{Nd(t)}$. Site 1184 samples have $\varepsilon_{Nd(t)}$ within in the range of Kwaimbaita-type basalt, yet show relatively large variations in both $^{87}Sr/^{86}Sr$ and $^{206}Pb/^{204}Pb$. We interpret these variations as being the result of secondary alteration that has changed the abundances of the fluid-mobile elements Rb, Sr, Pb and, to a certain extent, U. Site 1184 whole-rock data are from White *et al.* (2004). Data for fields taken from Mahoney (1987); Cheng *et al.* (1987); Castillo *et al.* (1991, 1994); Mahoney *et al.* (1991, 1993) and Tejada *et al.* (1996, 2002).

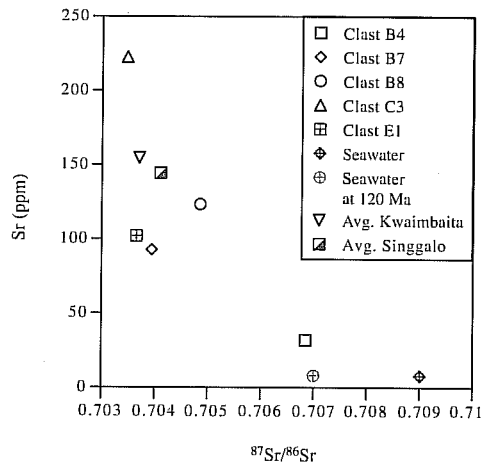

Fig. 8. Sr (unleached, ppm) v. $^{87}Sr/^{86}Sr$. The negative correlation suggests low Sr and high $^{87}Sr/^{86}Sr$ clasts have exchanged with sea water (8 ppm Sr and $^{87}Sr/^{86}Sr = 0.709$).

suggests that subaerial weathering of the volcaniclastic deposits did occur. However, Thordarson (2004) has shown that each volcaniclastic subunit probably represents a single eruptive event and, as such, soil could only have formed at the top of the subunits well away from the clasts. The Group 4 clasts were taken from a highly oxidized horizon of the core; they exhibit marked enrichments of Nb and Ta (as well as P_2O_5) and slight enrichments of Zr and Hf over the REE. Preferential mobilization of the LREE over the HREE (Ludden & Thompson 1979; Bach & Irber 1998; Kikawada *et al.* 2001) can explain the similarity between HREE abundances in the Group 2 clasts and those in average Kwaimbaita-type basalt (Fig. 6b) and the marked depletions and enrichments in the LREE and other incompatible elements. Enrichment of the LREE during alteration may also account for the Nb–Ta and Zr–Hf depletions relative to the REE in Group 2 Clast D1 (Fig. 6b) and Group 3 clast B5 (Fig. 6c).

In order to understand the nature of incompatible-element mobility during alteration, relatively immobile elements need to be identified for comparisons to be made. Kurtz *et al.* (2000) concluded that Nb and Ta were the most stable in the development of soils on volcanic terrains, but that Th, Zr and Hf were mobile during this process. The Site 1184 basalt clasts have $(Nb/Ta)_{PM}$ (primitive-mantle-normalized) ratios of 0.96 ± 0.06 (1σ) if Group 2 Clasts B2 ($(Nb/Ta)_{PM} = 0.51$) and B8 ($(Nb/Ta)_{PM} = 1.90$) are omitted. These two clasts exhibit quite dissimilar Nb abundances (2.24 and 6.56 ppm, respectively), yet similar Ta concentrations (0.25 and 0.20 ppm, respectively), and we conclude that at least in these two samples Nb was mobile. In examining the primitive-mantle-normalized patterns (Fig. 6a–d) our data set suggests that Ta was relatively immobile (note the narrow range of normalized Ta values in Fig. 6a–d, especially in the Group 2 patterns of

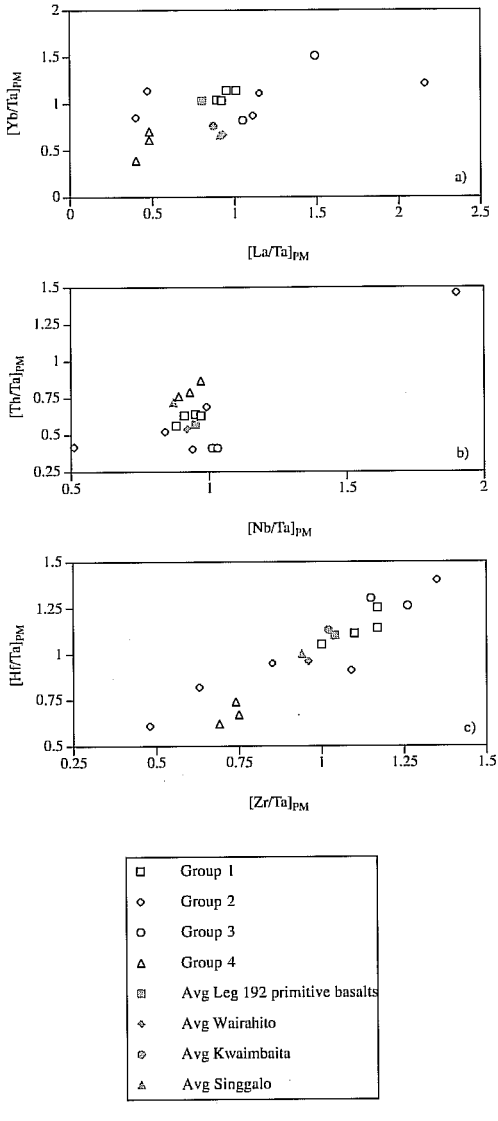

Fig. 9. (**a**) $(La/Ta)_{PM}$ v. $(Yb/Ta)_{PM}$; (**b**) $(Nb/Ta)_{PM}$ v. $(Th/Ta)_{PM}$; (**c**) $(Zr/Ta)_{PM}$ v. $(Hf/Ta)_{PM}$. The scatter in these plots away from typical OJP values is interpreted as showing the relative mobility of La, Yb, Nb, Th, Zr and Hf during alteration.

Fig. 6b). In an attempt to examine mobility, elements of interest (i.e. HFSE and REEs) have been normalized to Ta and compared with the average compositions of the Kwaimbaita, Singgalo, Wairahito and Kroenke-type basalts (Fig. 9a–c). The distribution seen in these figures is interpreted as primarily indicating mobility of La, Yb, Zr and Hf during alteration, although $(Yb/Ta)_{PM}$ values may be changed somewhat during fractional crystallization. Also, $(La/Ta)_{PM}$ ratios of most non-arc-related, mantle-derived magmas are relatively close to 1.0 (Sun & McDonough 1989; McDonough & Sun 1995). In magmas contaminated by continental crust, these values deviate from unity, but there is no evidence for such contamination in the OJP basalts (Mahoney 1987; Mahoney & Spencer 1991; Mahoney *et al.* 1993).

Assuming Ta is immobile, the relative mobility of other elements can be estimated. In terms of both light and heavy REE mobility, Group 1 clasts have similar $(La/Ta)_{PM}$ ratios to the average composition of each OJP basalt group, and slightly higher $(Yb/Ta)_{PM}$ ratios (Fig. 9a). Group 2 clasts exhibit a wide range of $(La/Ta)_{PM}$ values indicative of LREE enrichment and depletion, whereas $(Yb/Ta)_{PM}$ is more restricted. One Group 3 clast (Clast B5) is radically different from the average OJP basalts, suggesting that it may have been enriched in the REE. All Group 4 clasts have lower $(La/Ta)_{PM}$ and $(Yb/Ta)_{PM}$ values that overlap and extend to lower values than the average values for OJP basalts. Overall, these relationships are consistent with the altered nature of the Site 1184 clasts and with the observation that the LREE are more mobile than the HREE during alteration of basaltic material (e.g. Bach & Irber 1998).

The HFSE Zr, Nb, Hf and Th exhibit varying degrees of enrichment and depletion relative to Ta and the average compositions of OJP basalt types. As noted above, Nb appears immobile, except in two Group 2 clasts (Clasts B2 and B8), in which depletions and enrichments (respectively) relative to Ta are observed (Fig. 9b). All other clasts have $(Nb/Ta)_{PM}$ values *c.* 1.0, and in Figure 9b the Group 1 clasts plot directly on top of the average OJP basalt compositions, indicating that Nb/Ta ratios are unaffected by alteration. However, $(Th/Ta)_{PM}$ values for the remaining clasts are variable, with Group 2 clasts having the largest range (*c.* 0.4–1.5), which we interpret as indicating Th removal and addition relative to Ta. Whereas Th shows signs of mobility, it does not show nearly as much variation as La, Yb, Nb and Hf. Group 3 clasts have relative Th depletions, whereas those from Group 4 show slight Th enrichments (Fig. 9b). This contrasting behaviour between Groups 3 and 4 clasts is also seen in Figure 9c, where the Group 3 clasts are relatively enriched in Zr and Hf and those from Group 4 are depleted. Relative to the average OJP basalt compositions, Group 1 clasts appear to have a slight Zr enrichment (Fig. 9c). Again, Group 2 clasts exhibit a wide range of values.

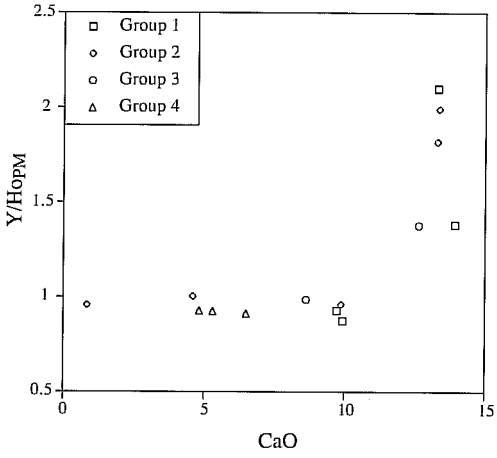

Fig. 10. CaO (wt%) v. $(Y/Ho)_{PM}$. $(Y/Ho)_{PM}$ is used to represent the positive Y anomaly present in five Site 1184 clasts. This anomaly is present in samples with CaO abundances over 10 wt%. This implies that the Y carrier is a Ca-rich phase, such as chabazite, a Ca-rich zeolite. See text for full details.

The presence of positive Y anomalies in five of the Site 1184 basalt clasts, as seen in their primitive-mantle-normalized incompatible-element plots (Fig. 6a–c), is puzzling. This could be the product of a polyatomic interference (e.g. $^{52}Cr^{37}Cl$, $^{70}Zn^{19}F$) that may have been induced through incomplete removal of HCl during our initial sample preparation or through incomplete HF removal during dissolution. However, these anomalies were replicated during different dissolutions ($HF–HNO_3$ acid and sodium peroxide fusion), so it is unlikely that an acid-induced polyatomic interference is the cause. Such positive Y anomalies are present in lavas that have undergone varying degrees of alteration (e.g. Kuschel & Smith 1992; Cotten *et al.* 1995). Past studies of element mobility during the weathering of igneous rocks have reported all of the REEs and Y as being collectively (although not uniformly) enriched or depleted in the weathered product (e.g. Duddy 1980; Marsh 1991; Price *et al.* 1991). Price *et al.* (1991) attributed these weathering effects to the presence or absence of secondary phosphates or clay minerals. Duddy (1980) concluded that the REE+Y were effectively immobilized by the development of vermiculite as a weathering product. Kuschel & Smith (1992) suggested the relative enrichment of Y was due solely to secondary phosphate and presented SEM images and mineral analyses of these phases in support of this conclusion, but generation of the positive Y anomaly in some of the weathered samples was not supported by the REE and Y contents of the secondary phosphates (i.e. no positive Y anomaly was present in these phases). However, Cotten *et al.* (1995) reported the presence of secondary rhabdophane-type REE–Y phosphates that did contain significant positive Y anomalies; the concentration of Y was of the order of 6–15 wt% Y_2O_3 (47 000–120 000 ppm Y). If such secondary phosphates were developed during the alteration of the Site 1184 basalt clasts, it is evident that only a minute amount would dramatically alter the Y abundance of the whole-rock composition. However, the REE are also enriched in these secondary phases (Cotten *et al.* 1995), but we see no concomitant REE enrichment in our clasts. In addition, there is no correlation between Y and P_2O_5 contents, and the samples with the highest P_2O_5 abundances exhibit no positive Y anomaly.

Only clasts with CaO >10 wt% exhibit a positive Y anomaly (represented as $(Y/Ho)_{PM}$) (Fig. 10). This indicates that the carrier of Y is rich in CaO. The Y carrier could, therefore, be calcite (present in thin section of some clasts) but there is no correlation between $(Y/Ho)_{PM}$ and LOI or between $(Y/Ho)_{PM}$ and Sr. Mahoney *et al.* (2001) reported the presence of zeolites in the Site 1184 volcaniclastic matrix. Our examination of thin sections of four of the samples that exhibit the positive Y anomaly (Clasts B3, B8, E1 and E2) shows that zeolite minerals are present as vesicle fill and veins both within and surrounding the clasts in the volcaniclastic matrix. If a Ca-rich zeolite (e.g. chabazite) was present in some of the basalt clasts, it could preferentially enrich the bulk composition in Y if significant interaction with sea water had occurred. For example, Wheat *et al.* (2002) noted that relative to ocean-ridge basalt, seawater exhibits a positive Y anomaly. Clast C1 contains zeolite minerals but does not show the Y anomaly. This sample has low CaO (4.83 wt%) and high Na_2O (5.73 wt%), suggesting that the zeolite present in Clast C1 is natrolite, a Na-rich zeolite. Formation of a Ca-rich zeolite during alteration by sea water in the other clasts with zeolites could produce a positive Y anomaly, as it appears that Na-rich zeolites are not Y carriers. Further work needs to be conducted in order to test this tentative conclusion.

In summary, we conclude that on the basis of primitive-mantle-normalized diagrams (Fig. 6a–d), Ta is the most immobile trace element in the suite of 14 basalt clasts studied from Site 1184. Niobium is generally immobile but two Group 2 clasts exhibit either Nb enrichment or depletion, indicating that Nb was mobilized

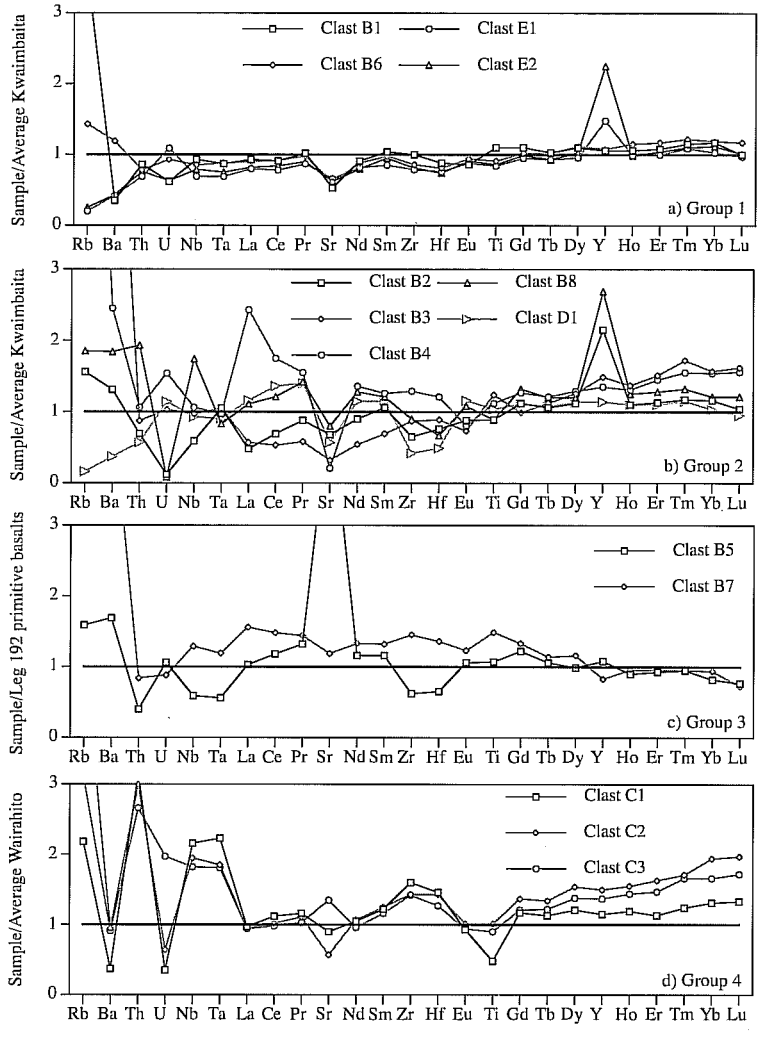

Fig. 11. (**a**) Group 1 basalt clasts normalized to average Kwaimbaita-type basalt; (**b**) Group 2 basalt clasts normalized to average Kwaimbaita-type basalt; (**c**) Group 3 basalt clasts normalized to average Kroenke-type basalt; and (**d**) Group 4 basalt clasts normalized to average Wairahito basalt. These profiles highlight the Site 1184 group affinities shown in Figure 6a–d. Data from which average basalt compositions were calculated are from Tejada *et al.* (1996, 2002), Neal *et al.* (1997), Birkhold (2000), Mahoney *et al.* (2001) and Fitton & Godard (2004).

during alteration. Zirconium and Hf also exhibit mobility and the LREE are more mobile than the HREE. Yttrium has been added to some clasts and is manifest as positive Y anomalies on Figure 6. We tentatively suggest that this is the result of secondary zeolite formation as a result of interaction of the clasts with sea water.

Petrogenetic interpretations

Although alteration has affected the major- and trace-element compositions of the Site 1184 basalt clasts, their incompatible-element profiles can help indicate similarities to other OJP basalt types (Fig. 6a–d). In order to highlight these similarities, we have also normalized data for each of the clasts from Groups 1–4 to the OJP basalt types to which they are most similar (Fig. 11a–d). Group 1 clasts show clear similarities to Kwaimbaita-type basalt (Neal *et al.* 1997; Tejada *et al.* 2002). Depletions in Rb and Ba and variable U concentrations can be attributed to alteration (Seyfried *et al.* 1998). The relatively low Sr abundances in these clasts relative to the

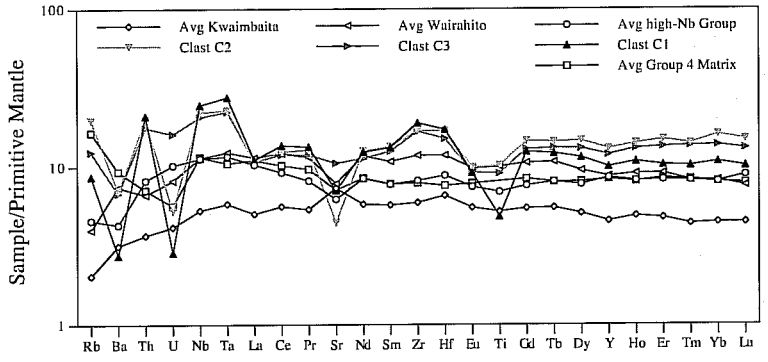

Fig. 12. Average Group 4 clast composition, average Group 4 volcaniclastic matrix composition, average high-Nb group of Fitton & Godard (2004), and average Kwaimbaita-type basalt, all normalized to primitive mantle. Note the similarities in the high-Nb group to the Group 4 volcaniclastic matrix and the significant difference of that to the Group 4 clasts. However, the incompatible-element profiles are similar (enriched Nb and Ta over the LREE), although distinct differences do occur (such as the significant depletion in Eu and Ti in the Group 4 clasts). These data are interpreted to mean that the Group 4 matrix and clasts are not from the same eruptive episode, yet they are probably related, as they both represent a distinctive high-Nb magma type not seen before on the OJP.

average Kwaimbaita-type basalt may be a result of greater amount of plagioclase fractionation in the Site 1184 magmas, but there is no corresponding Eu depletion (Figs 6a and 11a). It is much more likely to be due to preferential Sr removal during alteration. The Group 2 clasts, the most variable group, are tentatively interpreted to be akin to the Kwaimbaita-type basalt on the basis of ε_{Nd} and HREE abundances (Figs 6b and 11b). Group 2 clasts are slightly more enriched in the HREE than are the average Kwaimbaita-type basalt, and elements more incompatible than Ti in Figure 11b are highly variable (Fig. 11b). However, Ta exhibits little variation, as does Nb (except for Clasts B2 and B8; see above), and values of these two elements are similar to the Ta and Nb values of the Kwaimbaita-type basalt (Group 2 Ta = 0.20–0.25 ppm v. 0.24 ppm for the average Kwaimbaita-type basalt). The two clasts that make up Group 3 are broadly similar to the Kroenke-type basalts (Fig. 11c), although Clast B7 has Ti, Zr and Nb concentrations similar to those of average Kwaimbaita-type basalt. Clast B5 exhibits the greatest variability with depletions in Nb, Ta, Zr and Hf, and a large enrichment in Sr. Clast B7 appears to be intermediate between Kroenke-type and Kwaimbaita-type basalt compositions. Finally, Group 4 clasts are more evolved than the Wairahito basalts (the most evolved rock type so far recorded from the OJP) of Birkhold (2000), and are significantly enriched in Th, Nb, Ta and the HREE relative to average Wairahito basalt. This group also displays negative Eu and Ti anomalies (Figs 6d and 11d), and clasts forming this group have the highest LOI values (*c.* 7.2–11.8 wt%). These samples have similarly shaped profiles to the whole-rock analyses of those of four samples of bulk tuff from Subunit IIC (high-Nb group, Fitton & Godard 2004), although they are significantly more enriched than the high-Nb group. However, analysis of the volcaniclastic matrix surrounding the clasts from Subunit IIC shows strong similarities to the high-Nb group (Fig. 12). The compositional differences between the Group 4 clasts and the high-Nb group and Group 4 matrix indicate that the clasts and matrix were not formed during the same eruptive episode, although they are probably related because they both show high Nb, Ta and Th relative to the REE, which is unique among OJP samples. The Group 4 basalt clasts and matrix and the high-Nb group of Fitton & Godard (2004) represent a magma type not seen elsewhere in the region.

Source region

Compositions of unaltered glass present in the lower sections of the Site 1184 core are similar to those of the widespread Kwaimbaita-type lavas (White *et al.* 2004). The basalt clasts studied here define a narrow range of initial $\varepsilon_{Nd(t)}$ values from +6.0 to +6.5, within the field defined by the Kwaimbaita-type basalt (Mahoney 1987; Mahoney *et al.* 1993; Tejada *et al.* 1996, 2002, 2004). Combining this observation with similarities in normalized incompatible element profiles, we suggest that Groups 1–4 were derived

from the Kwaimbaita-type source, and represent basalts with affinities to both the Kwaimbaita-type and the MgO-rich Kroenke-type basalts (e.g. Mahoney *et al.* 2001; Tejada *et al.* 1996, 2002, 2004). Group 4 clasts are relatively evolved, more so than any other lava type yet recovered from the OJP, and thus are unique OJP samples. However, the similarity of Nd isotopic ratios with those of the Kwaimbaita- and Kroenke-type basalts indicates derivation from an isotopically similar or identical source (Tejada *et al.* 2002, 2004).

Summary and conclusions

Ocean Drilling Program Leg 192 recovered the first evidence that at least part of the eastern salient of the Ontong Java Plateau was erupted at or above sea level. Unlike the OJP basalt sequence cored at ODP Leg 130 Site 807, and the now subaerial outcrops on Malaita and Santa Isabel (Solomon Islands), the Singgalo type of basalt flows is absent.

Major-element, trace-element and isotope variations within the suite of basalt clasts extracted from the volcaniclastic sequence at Site 1184 show the effects of secondary alteration on basalt derived from the Kwaimbaita-type mantle source. On the basis of incompatible-element profiles (normalized to estimated primitive mantle values), four groups of clasts are defined. Most of the clasts (Groups 1 and 2) have affinities with Kwaimbaita-type basalt, but two show some similarities to the relatively Mg-rich Kroenke-type lavas (Group 3). The three Group 4 clasts are unique among samples recovered from the OJP in that their incompatible-element abundances are relatively enriched. Secondary alteration has mobilized elements that are immobile during moderate alteration, namely Zr, Hf, Th, the REE and, in two clasts, Nb. Of the HFSE, only Ta appears unaffected by this secondary alteration. Several samples also exhibit curious positive Y anomalies, which we tentatively interpret to be the result of secondary Ca-rich zeolite (chabazite?) development through interaction with sea water.

Ages estimated for the Site 1184 sequence from ^{40}Ar–^{39}Ar measurements (Chambers *et al.* 2004) strongly suggest that the eastern salient formed concurrently with the high plateau and that there is not a younging trend from the high plateau to the eastern salient (Kroenke & Mahoney 1996). Evidence for emergence of a portion of the plateau during its formation has potentially important implications for the effects of OJP emplacement on the local and, perhaps, global environment during the Aptian, the magnitude of which must be addressed by future drilling expeditions to the OJP and other parts of the western Pacific. Furthermore, the discovery that the Kwaimbaita-type source was also producing basaltic volcanism both on the main plateau and on the eastern salient has important implications for the modelling of magma dynamics and evolution during the growth of the OJP.

This research used samples provided by the Ocean Drilling Program (ODP). ODP is sponsored by the US National Science Foundation (NSF) and participating countries under management of Joint Oceanographic Institutions (JOI), Inc. Funding for this research was provided by USSSP to C. R. Neal and P. R. Castillo. We would like to thank D. Birdsell of the Center for Environmental Science and Technology at the University of Notre Dame for his help with the ICP-OES analyses. We would also like to thank reviewers P. Wallace, S. Revillon and G. Fitton, as well as one anonymous reviewer, for their helpful comments and suggestions.

References

BACH, W. & IRBER, W. 1998. Rare earth element mobility in the oceanic lower sheeted dyke complex: evidence from geochemical data and leaching experiments. *Chemical Geology*, **151**, 309–326.

BERGEN, J.A. 2004. Calcareous nanofossils from ODP Leg 192, Ontong Java Plateau. *In*: FITTON, J.G., MAHONEY, J.J., WALLACE, P.J. & SAUNDERS, A.D. (eds) *Origin and Evolution of the Ontong Java Plateau*. Geological Society, London, Special Publications, **229**, 113–132.

BIENVENU, P., BOUGAULT, H., JORON, J.L., TREUIL, M. & DMITRIEV, L. 1990. MORB alteration; rare-earth element/ non-rare-earth hygromagmaphile element fractionation. *Chemical Geology*, **82**, 1–14.

BIRKHOLD, A.L. 2000. *A geochemical investigation of Ontong Java Plateau basement exposed on the Island of Makira (San Cristobal), Solomon Islands, South Pacific.* PhD Thesis, University of Notre Dame.

CASTILLO, P.R., CARLSON, R.W. & BATIZA, R. 1991. Origin of the Nauru Basin igneous complex: Sr, Nd, and Pb isotope and REE constraints. *Earth and Planetary Science Letters*, **103**, 200–213.

CASTILLO, P.R., PRINGLE, M.S. & CARLSON, R.W. 1994. East Mariana Basin Tholeiites: Cretaceous intraplate basalts or rift basalts related to the Ontong Java plume? *Earth and Planetary Science Letters*, **123**, 139–154.

CHAMBERS, L.M., PRINGLE, M.S. & FITTON, J.G. 2004. Phreatomagmatic eruptions on the Ontong Java Plateau: an Aptian $^{40}Ar/^{39}Ar$ age for volcaniclastic rocks at ODP Site 1184. *In*: FITTON, J.G., MAHONEY, J.J., WALLACE, P.J. & SAUNDERS, A.D. (eds) *Origin and Evolution of the Ontong Java Plateau*. Geological Society, London, Special Publications, **229**, 325–331.

CHENG, Q., PARK, K.H., MACDOUGALL, J.D., ZINDLER, A., LUGMAIR, G.W., STAUDIGEL, H., HAWKINS, J.W.

& LONSDALE, P.F. 1987. Isotopic evidence for a hotspot origin of the Louisville seamount chain. *In*: KEATING, B.H., FRYER, P., BATIZA, R. & BOEHLERT, G.W. (eds) *Seamounts, Islands, and Atolls.* American Geophysical Union, Geophysical Monograph, **43**, 283–296.

COTTEN, J., LE DEZ, A., BAU, M., CAROFF, M., MAURY, R.C., DULSKI, P., FOURCADE, S., BOHN, M. & BROUSSE, R. 1995. Origin of anomalous rare-earth element and yttrium enrichments in subaerially exposed basalts: Evidence from French Polynesia. *Chemical Geology*, **119**, 115–138.

DEPAOLO, D.J. & INGRAM, B.L. 1985. High-resolution stratigraphy with Sr isotopes. *Science*, **227**, 938–941.

DUDDY, I.R. 1980. Redistribution and fractionation of rare-earth and other elements in a weathered profile. *Chemical Geology*, **30**, 363–381.

FITTON, J.G & GODARD, M. 2004. Origin and evolution of magmas on the Ontong Java Plateau. *In*: FITTON, J.G., MAHONEY, J.J., WALLACE, P.J. & SAUNDERS, A.D. (eds) *Origin and Evolution of the Ontong Java Plateau.* Geological Society, London, Special Publications, **229**, 151–178.

FLANAGAN, F.J. 1984. Three USGS mafic rock reference samples, W-2, DNC-1, and BIR-1. *US Geological Survey Bulletin*, **1623**, 54.

GLADNEY, E.S. & ROELANDTS, I. 1988. 1987 compilation of elemental concentration data for USGS BIR-1, DNC-1, and W-2. *Geostandards Newsletter*, **12**, 63–118.

GOVINDARAJU, K. 1994. 1994 compilation of working values and descriptions for 383 geostandards. *Geostandards Newsletter*, **118**, 1–158.

HART, R. 1970. Chemical exchange between sea water and deep ocean basalts. *Earth and Planetary Science Letters*, **9**, 269–279.

HART, S.R., ERLANK, A.J. & KABLE, E.J.D. 1974. Sea floor basalt alteration: Some chemical and Sr isotopic effects. *Contributions to Mineralogy and Petrology*, **44**, 219–230.

HESS, J., BENDER, M.L. & SCHILLING, J.-G. 1986. Evolution of the ratio of strontium-87 to strontium-86 in seawater from Cretaceous to present. *Science*, **231**, 979–984.

JANNEY, P.E. & CASTILLO, P.R. 1996. Basalts from the central Pacific Basin; evidence for the origin of Cretaceous igneous complexes in the Jurassic western Pacific. *Journal of Geophysical Research, B, Solid Earth and Planets*, **101**, 2875–2893.

KIKAWADA, Y., OSSAKA, T., OI, T. & HONDA, T. 2001. Experimental studies on the mobility of Lanthanides accompanying alteration by acidic hot spring water. *Chemical Geology*, **176**, 137–149.

KROENKE, L.W. & MAHONEY, J.J. 1996. Rifting of the Ontong Java Plateau's eastern salient and seafloor spreading in the Ellice Basin; relation to the 90 Ma eruptive episode on the plateau. *Eos, Transactions of the American Geophysical Union*, **77**, 713.

KURTZ, A.C., DERRY, L.A., CHADWICK, O.A. & ALFANO, M.J. 2000. Refractory element mobility in volcanic soils. *Geology*, **28**, 683–686.

KUSCHEL, E. & SMITH, I.E.M. 1992. Rare earth mobility in young arc-type volcanic rocks from northern New Zealand. *Geochimica et Cosmochimica*, **56**, 3951–3955.

LE BAS, M.J., LE MAITRE, R.W., STRECKEISEN, A. & ZANETTIN, B.A. 1986. Chemical Classification of igneous rocks based on the total alkali-silica diagram. *Journal of Petrology*, **27**, 745–750.

LONGERICH, H.P., JENNER, G.A., FRYER, B.J. & JACKSON, S.E. 1990. Inductively coupled plasma-mass spectrometric analysis of geological samples: A critical evaluation based on case studies. *Chemical Geology*, **83**, 105–118.

LUDDEN, J.N. & THOMPSON, G. 1979. An evaluation of the behavior of the rare earth elements during the weathering of sea-floor basalt. *Earth and Planetary Science Letters*, **43**, 85–92.

LUGMAIR, G.W. & GALER, S.J.G. 1992. Age and isotopic relationships among the angrites Lewis Cliff 86010 and Angra dos Reis. *Geochimica et Cosmochimica*, **56**, 1673–1694.

MACDONALD, G.A. & KATSURA, T. 1964. Chemical composition of Hawaiian lavas. *Journal of Petrology*, **5**, 82–133.

MAHONEY, J.J. 1987. An isotopic survey of Pacific oceanic plateaus: implications for their nature and origin. *In*: KEATING, B.H., FRYER, P., BATIZA, R. & BOEHLERT, G.W. (eds) *Seamounts, Islands, and Atolls.* American Geophysical Union, Geophysical Monograph, **43**, 207–220.

MAHONEY, J.J. & SPENCER, K.J. 1991. Isotopic evidence for the origin of the Manihiki and Ontong Java oceanic plateaus. *Earth and Planetary Science Letters*, **104**, 196–210.

MAHONEY, J.J., STOREY, M., DUNCAN, R.A., SPENCER, K.J. & PRINGLE, M.S. 1993. Geochemistry and age of the Ontong Java Plateau. *In*: PRINGLE, M.S., SAGER, W.W., SLITER, W.V. & STEIN, S. (eds) *The Mesozoic Pacific: Geology, Tectonics, and Volcanism.* American Geophysical Union, Geophysical Monograph, **77**, 233–262.

MAHONEY, J.J., FITTON, J.G., WALLACE, P.J. *et al.* 2001. *Proceedings of the Ocean Drilling Program, Initial Reports*, **192** (CD-ROM). Available from: Ocean Drilling Program, Texas A&M University, College Station TX 77845–9547, USA.

MARSH, J.S. 1991. REE fractionation and Ce anomalies in weathered Karoo dolerite. *Chemical Geology*, **90**, 189–194.

MCDONOUGH, W.F. & SUN, S.-S. 1995. The composition of the Earth. *Chemical Geology*, **120**, 223–253.

MENZIES, M. & SEYFRIED, W.E. 1979. Basalt–seawater interaction; trace element and strontium isotopic variations in experimentally altered glassy basalt. *Earth and Planetary Science Letters*, **44**, 463–472.

NEAL, C.R. 2001. The interior of the Moon: The presence of garnet in the primitive, deep lunar mantle. *Journal of Geophysical Research, B, Solid Earth and Planets*, **106**, 27 865–27 885.

NEAL, C.R., MAHONEY, J.J., KROENKE, L.W., DUNCAN, R.A. & PETTERSON, M.G. 1997. The Ontong Java Plateau. *In*: MAHONEY, J.J. & COFFIN, M.F. (eds) *Large Igneous Provinces: Continental, Oceanic, and Planetary Flood Volcanism.* American Geophysical Union, Geophysical Monograph, **100**, 183–216.

PRICE, R.C., GRAY, C.M., WILSON, R.E., FREY, F.A. & TAYLOR, S.R. 1991. The effects of weathering on rare-earth element, Y and Ba abundances in Tertiary basalts from southeastern Australia. *Chemical Geology*, **93**, 245–265.

RICHARDS, M.A., DUNCAN, R.A. & COURTILLOT, V. 1989. Flood basalts and hot-spot tracks: plume heads and tails. *Science*, **246**, 103–107.

SEYFRIED, W.E, CHEN, X. & CHAN, L.H. 1998. Trace element mobility and lithium exchange during hydrothermal alteration of seafloor weathered basalt; an experimental study at 350 degrees, 500 bars. *Geochimica et Cosmochimica Acta*, **62**, 949–960.

SIKORA, P.J. & BERGEN, J.A. 2004. Lower Cretaceous planktonic foraminiferal and nannofossil biostratigraphy of Ontong Java sites from DSDP Leg 30 and ODP Leg 192. *In*: FITTON, J.G., MAHONEY, J.J., WALLACE, P.J. & SAUNDERS, A.D. (eds) *Origin and Evolution of the Ontong Java Plateau*. Geological Society, London, Special Publications, **229**, 83–111.

SUN, S.-S. & MCDONOUGH, W.F. 1989. Chemical and isotopic systematics of oceanic basalts: implications for mantle composition and processes. *In*: SAUNDERS A.D. & NORRY, M.J. (eds) *Magmatism in the Ocean Basins*. Geological Society, London, Special Publications, **42**, 313–345.

TEJADA, M.L.G., MAHONEY, J.J., DUNCAN, R.A. & HAWKINS, M.P. 1996. Age and geochemistry of basement and alkalic rocks of Malaita and Santa Isabel, Solomon Islands, southern margin of Ontong Java Plateau. *Journal of Petrology*, **17**, 361–393.

TEJADA, M.L.G., MAHONEY, J.J., NEAL, C.R., DUNCAN, R.A. & PETTERSON, M.G. 2002. Basement geochemistry and geochronology of Central Malaita, Solomon Islands, with implications for the origin and evolution of the Ontong Java Plateau. *Journal of Petrology*, **43**, 449–484.

TEJADA, M.L.G., MAHONEY, J.J., CASTILLO, P.R., INGLE, S.P., SHETH, H.C. & WEIS, D. 2004. Pin-pricking the elephant: evidence on the origin of Ontong Java Plateau from Pb–Sr–Hf–Nd isotopic characteristics of ODP Leg 192 basalts. *In*: FITTON, J.G., MAHONEY, J.J., WALLACE, P.J. & SAUNDERS, A.D. (eds) *Origin and Evolution of the Ontong Java Plateau*. Geological Society, London, Special Publications, **229**, 133–150.

THORDARSON, T. 2004. Accretionary-lapilli-bearing pyroclastic rocks at ODP Leg 192 Site 1184: a record of subaerial phreatomagmatic eruptions on the Ontong Java Plateau. *In*: FITTON, J.G., MAHONEY, J.J., WALLACE, P.J. & SAUNDERS, A.D. (eds) *Origin and Evolution of the Ontong Java Plateau*. Geological Society, London, Special Publications, **229**, 275–306.

TODT, W., CLIFF, R.A., HANSER, A. & HOFMANN, A.W. 1996. Evaluation of a ^{202}Pb+^{205}Pb double spike for high-precision lead isotopic analysis. *In*: BASU, A. & HART, S. (eds) *Earth Processes: Reading the Isotopic Code*. American Geophysical Union, Geophysical Monograph, **95**, 429–437.

WHEAT, C.G., MOTTL, M.J. & RUDNICKI, M. 2002. Trace element and REE composition of a low-temperature ridge-flank hydrothermal spring. *Geochimica et Cosmochimica*, **66**, 3693–3705.

WHITE, R., CASTILLO, P.R., NEAL, C.R., FITTON, J.G. & GODARD, M. 2004. Phreatomagmatic eruptions on the Ontong Java Plateau: chemical and isotopic relationship to Ontong Java Plateau basalts. *In*: FITTON, J.G., MAHONEY, J.J., WALLACE, P.J. & SAUNDERS, A.D. (eds) *Origin and Evolution of the Ontong Java Plateau*. Geological Society, London, Special Publications, **229**, 307–323.

WILSON, S.A. 1997. *Data Compilation for USGS Reference Material BHVO-2, Hawaiian Basalt*. US Geological Survey, Open-File Report, in prep. Available online at: http//minerals.cr.usgs.gov/geo_chem_stand/basaltbhv02.html.

WINCHESTER, J.A. & FLOYD, P.A. 1976. Geochemical magma type discrimination: Application to altered and metamorphosed basic igneous rocks. *Earth and Planetary Science Letters*, **28**, 459–469.

YAN, C.Y. & KROENKE, L.W. 1993. A plate tectonic reconstruction of the Southwest Pacific, 100–0 Ma. *In*: BERGER, W.H., KROENKE, L.W., MAYER, L.A. *et al.* (eds) *Proceedings of the Ocean Drilling Program, Scientific Results*, **130**, 697–709.